Chapter 4

Adaptation to natural time series of intensities

ABSTRACT

In natural conditions, an organism copes with the large variations of the luminance input to the eyes by means of adaptation. Here, we investigate the luminance and contrast adaptation mechanisms under natural conditions, using a time series of intensities representative of what a photoreceptor would encounter while moving in a natural environment. We measured psychophysical detection thresholds for 1-second luminance increments relative to the natural time series, in comparison to stimuli with different dynamics. For the natural time series we found a threshold that is elevated about 20% above steady-state level. Thresholds for various stimuli vary approximately linearly with stimulus contrast, and are consistent with mediation by the parvocellular pathway. Detection thresholds increase with decreasing test duration, depending on stimulus type.

INTRODUCTION

When an organism moves around in a natural environment, the luminance input to the eyes changes continually. The input luminance range is much larger than the (linear) dynamic range of photoreceptors and subsequent neurons (e.g., van Hateren, 1997). The visual system copes with this problem by means of luminance and contrast adaptation. These adaptation mechanisms have been studied extensively, both psychophysically (e.g., Hayhoe *et al*., 1992; Foley & Boynton, 1993; Kortum & Geisler, 1995; Hood *et al*., 1997; Pokorny & Smith, 1997; Poot *et al*., 1997) and physiologically (e.g., Donner *et al*., 1990; Lankheet *et al*., 1993; Wu & Burns, 1996; Yeh *et al*., 1996; Shapley, 1997; Victor *et al*., 1997). Although these studies are giving an increasingly detailed view of early processes of luminance and contrast adaptation, it is not clear how these processes act in concert under natural luminance conditions.

Here we study how the human visual system handles natural luminance and contrast variations through adaptation, by performing psychophysical experiments using a natural time series of intensities (NTSI). As described in the section 'Natural time series of intensities', and by van Hateren (1997), NTSIs were measured with a light detector carried on the head by a freely walking person. In the present study, we probe the sensitivity of the visual system during presentation of the NTSI by measuring detection thresholds for small luminance increments relative to the NTSI. This experiment gives

---

Based on: L. Poot, J.H. van Hateren & H.P. Snippe. Adaptation to natural time series of intensities. In preparation

information on how well sensitivity is retained during the rapid luminance fluctuations of the NTSI, and to what extent the early processing channels are saturated. Furthermore, detection of small luminance increments is a relevant task for natural vision, since detection of, for example, the shape or motion of objects depends on the ability to discriminate small luminance differences.

For the psychophysical experiments we made several simplifying choices. First, the NTSI was presented in a large, spatially homogeneous way, in order to produce a well-defined adaptation condition, which is not compromised by eye movements. This stimulus probably produces sensitivity changes reasonably close to those in natural circumstances, since at least luminance adaptation occurs locally in the retina, possibly at the scale of a cone's receptive field (Chaparro *et al*., 1995; He & MacLeod, 1998). Second, a relatively long test duration was chosen to integrate the statistics of the natural time series, and thus to reduce the total measuring time for the experiment. Also the recording of the NTSIs was subject to simplifying choices. Most importantly, eye movements were not taken into account, and a choice had to be made for the task of the person wearing the light detector during recording. This is discussed further in the section 'Relevance for natural vision'.

Given these simplifications, the present article should be considered as a first approach towards studying luminance and contrast adaptation during normal behaviour in natural luminance conditions. Eventually, a full spatio-temporal study should be performed once calibrated spatio-temporal stimuli and display equipment of sufficient dynamic range become available.

NATURAL TIME SERIES OF INTENSITIES

Recording method

A more complete and detailed description of the method for recording NTSIs can be found in van Hateren (1997). Here, we will briefly summarize this method. To measure luminances we constructed a small detector, consisting of a lens, colour filters, a pinhole in front of a light guide, and at the other end of the light guide a photomultiplier with a linear intensity-response characteristic. This detector has spatial and spectral properties similar to those of (para)foveal human cones: its spectral sensitivity is not very different from the photopic sensitivity of the human eye and it has an angular resolution of a few arcminutes. Signals from the photomultiplier were stored on a portable DAT-recorder, and off-line reduced to either 1200 samples/s (Fig. 1 and Table 1) or 400 samples/s (psychophysical experiments), both by block averaging.

The detector was mounted on a head-band, which was worn by a freely walking person during recording. The device followed the direction of gaze of the head, thus eye movements are not accounted for. Also accounting for eye movements during free walking would be technically very demanding. To avoid gross mismatches between the gaze directions of the eyes and the detector, the subjects wore marked glasses, and were

instructed to keep the markers at a fixed position in the visual field, i.e. relative to the retina. Gaze was thus mostly shifted by moving the head instead of the eyes. Although this is obviously only a crude way to obtain time series of intensities relevant for small groups of photoreceptors, we believe the statistics of the time series is not too strongly dependent on the method of recording. As a control, we recorded a time series while carrying the system in hand and shifting its pointing direction regularly; this gave similar results as the head-based measurements. Although one might presume that precise stabilization of the eyes' gaze should influence the results strongly, this can at most be the case for the very central parts of the visual field: during free walking, most of the visual field is not stabilized at all.

Time series properties

Six different subjects measured a total of 12 NTSIs during 45-minute walks through various mixed environments of meadows and woods. Weather conditions ranged from sunny to foggy. In this section we will present some of the characteristic properties of these NTSIs (Table 1). Results from two NTSIs obtained with quite different weather conditions are further presented in Fig. 1.

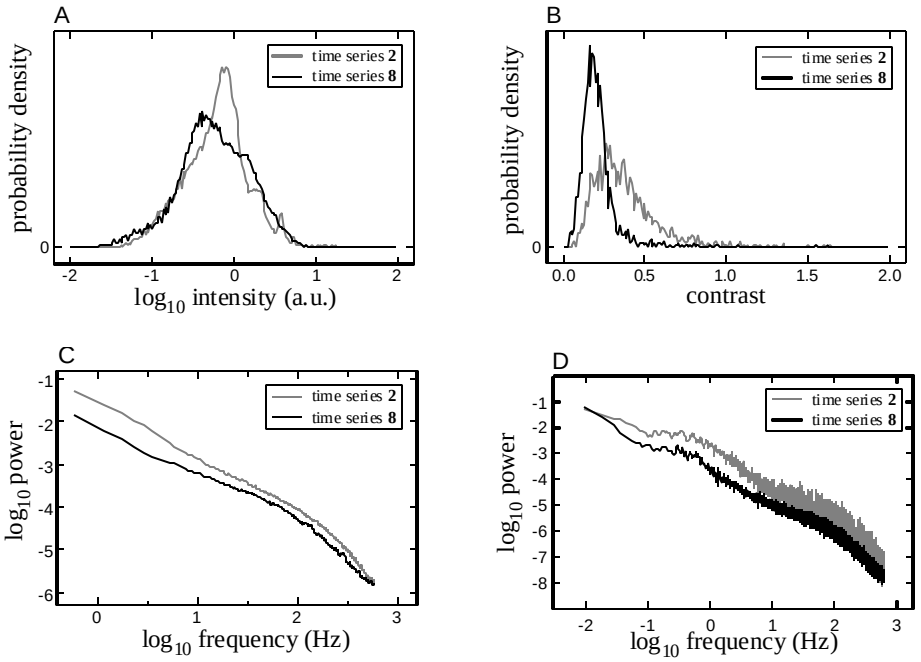

Figure 1. Properties of two natural time series of intensities. Number 2 was recorded on a sunny day, number 8 on a foggy day. A: Intensity distributions for these two time series. B: Distributions of contrast in the frequency range 0.6-100 Hz. C: Power spectra on a log-log scale, in the frequency range 0.6-600 Hz. D: Power spectra in the frequency range 0.009-600 Hz.

Time series number	contrast 0.6-100 Hz	contrast 0.009-100 Hz	β 0.6-100 Hz	β 0.009-100 Hz	weather
1	0.41 ± 0.21	0.72 ± 0.23	0.96 ± 0.01	0.98 ± 0.02	sunny
2	0.39 ± 0.20	0.82 ± 0.54	1.21 ± 0.01	0.57 ± 0.03	sunny, slightly hazy
3	0.41 ± 0.28	0.94 ± 0.44	1.16 ± 0.01	0.45 ± 0.02	sunny, scattered clouds
4	0.56 ± 0.37	1.01 ± 0.43	1.36 ± 0.01	0.82 ± 0.03	sunny, scattered clouds
5	0.49 ± 0.37	1.64 ± 0.97	1.05 ± 0.01	0.64 ± 0.03	sunny, scattered clouds
6	0.26 ± 0.16	0.65 ± 0.69	1.18 ± 0.01	0.47 ± 0.03	sunny, scattered clouds
7	0.34 ± 0.21	0.87 ± 0.45	1.20 ± 0.01	0.94 ± 0.03	foggy
8	0.23 ± 0.12	0.49 ± 0.20	1.00 ± 0.01	0.92 ± 0.04	foggy
9	0.27 ± 0.19	0.80 ± 0.82	1.45 ± 0.02	0.78 ± 0.03	clouded
10	0.29 ± 0.27	0.62 ± 0.43	1.26 ± 0.01	0.68 ± 0.03	clouded, later diffuse sun
11	0.41 ± 0.29	1.42 ± 0.65	1.33 ± 0.01	0.71 ± 0.03	clouded, hazy, grey
12	0.29 ± 0.16	0.76 ± 0.67	1.14 ± 0.01	0.69 ± 0.04	clouded, hazy, grey

Table 1 Properties of a number of NTSIs measured in mixed environments with mixed weather conditions.

In Fig. 1 A, the probability density of intensity for both time series is shown. Note that the roughly symmetrical distribution on a log scale means that the distribution is very skew on a linear scale: most intensities are low, but there is a long tail containing high intensity peaks. The distribution of intensities is quite broad: values typically occupy a range of about 2.5-3 log units.

In the second and third columns of Table 1, the calculated contrast for each of the time series is shown, for two different temporal bandwidths (0.6-100 Hz and 0.09-100 Hz). Contrast was calculated for consecutive stretches of the NTSI, by calculating the power spectrum (see Figs 1 C and D) of each stretch and subsequently integrating the power contained within the chosen bandwidth. The square root of this value was then divided by the dc-term (the average of each stretch). The contrast value given in the table is the average (± the standard deviation) of all stretches of an NTSI. Histograms of these values (of 0.6-100 Hz bandwidth) are shown in Fig. 1 B. Contrast averages of the 12 NTSIs range between 0.23 and 0.56 for the 0.6-100 Hz bandwidth, and between 0.49 and 1.64 for the 0.009-100 Hz bandwidth. As can be expected, foggy and cloudy weather in general lead to smaller contrasts than sunny weather, although Table 1 also shows an appreciable variation. In Figure 1 B it can be seen that the distribution of contrast values for time series number 2 (sunny) is shifted to higher contrasts than time series number 8 (foggy). The distribution for number 2 is also broader than for number 8, which means that there is more variation in contrast. Comparing the contrasts for the two different bandwidths in Table 1, we see that a larger bandwidth leads to higher contrast. This is caused by the fact that low-frequency fluctuations also add to the contrast of the 0.009-100 Hz bandwidth.

Figures 1 C and D show power spectra for two of the NTSIs, at two different bandwidths (C: 0.6-600 Hz; D: 0.09-600 Hz). Spectra were calculated from consecutive stretches (of 1.7 s for the small bandwidth, and 110 s for the large bandwidth) of the complete time series, and subsequently averaged. The power spectra approximately follow a more or less straight line on a log-log scale, which means that they behave as $1/f_t^{\beta}$, with f_t the temporal frequency and β a constant. Columns 4 and 5 of Table 1 show the values of β obtained from fits to the spectra up to 100 Hz; β is roughly 1. This approximate $1/f_t$ behaviour of natural time series can be shown to be consistent with the approximate $1/f_s^2$ behaviour of the spatial power spectrum of natural images, as was explained earlier by van Hateren (1997). For frequencies higher than about 100 Hz, the power spectrum starts to deviate from a straight line, because the spatial aperture of the light detector has low-pass filtering characteristics as the subject carrying the detector produces limited angular velocities. For frequencies below about 0.5 Hz the power spectrum flattens which results in a lower value of β for the higher bandwidth. This flattening of the spectrum indicates a breakdown of scale-invariance for very low spatio-temporal frequencies. The spectrum of time series number 2 lies above that of time series number 8 for the complete frequency range. This means that the spectrum contains more power, which is consistent with the fact that time series number 2 has a higher contrast (Fig. 1 B).

We performed the psychophysical experiments with a time stretch of one minute chosen from time series number 1. This minute contains a typical variation in intensity and contrast and is therefore representative for NTSIs in general.

RELEVANCE FOR NATURAL VISION

After having described the properties of the NTSI, the question remains how representative this time series is for the dynamics of the visual input under natural circumstances. First, the recording equipment of the NTSI follows the head movements, but not the eye movements of the person wearing the headband. The dynamics of these movements are rather different. The eyes make short, rapid saccades (eye velocity up to 700 deg/s) and try to stabilize the retinal image in between saccades (Carpenter, 1977), whereas head movements are slower (up to 100 deg/s) and more continuous (Kowler *et al*., 1992; Grasso *et al*., 1998). In our opinion this is not a major concern. Since the person wearing the headband navigated through an outdoors environment, the luminance input for each photoreceptor changed continuously. Even when the fovea is fixating on a certain object, there still are luminance fluctuations on most photoreceptors due to the optic flow generated by moving through an environment with depth structure (Koenderink, 1986; Cornilleau-Pérès & Gielen, 1996). Furthermore, it is not known how well the eyes actually stabilize an image on the retina in between saccades, when a person is moving around naturally. Even when a person is sitting down, and is only allowed to move the upper body, stabilization is far from perfect (Epelboim, 1998). This was particularly the case when a task was performed which involved movements of the arms, where retinal image velocities of up to 5 deg/s were found. During a navigation task the retinal image velocity might even be higher. We can thus say that although time series with and without eye movements must be different, this difference is probably not as large during navigation as it may seem at first glance.

This conclusion leads to another important question: how does the task performed by the person carrying the recording equipment influence the measured time series and how would this influence our results? For these psychophysical experiments we chose to record an NTSI during a navigation task, because this is one of the important activities that have shaped our visual system. Another possible task could be one where a better visual accuracy is needed, for instance using tools or reading. These tasks will result in a different NTSI, the main difference coming from the fact that body motions are rather small during these tasks, and eye movements are then producing the majority of changes in the retinal image. Combined with the fact that the environment does not usually change in such tasks, we can expect an NTSI with longer periods of roughly stable intensity, with rapid transitions between them during saccades. This is also interesting to investigate, but it would need a recording method for the time series that does follow eye movements. The specific psychophysical results presented here may not be generally applicable to these kinds of tasks. But we can say that, when studying adaptation, the outdoors navigation task is more demanding for the adaptation processes in the early visual system, since in that case large luminance fluctuations continuously occur. Thus, if we find that the adaptation mechanism is able to handle the navigation NTSI, it will probably also be able to handle NTSIs recorded during other tasks.

The psychophysical task in these experiments was not designed to be naturalistic as such, but had the main purpose of probing the adaptation state of the visual system at various times during presentation of a naturalistic stimulus. To start with, we chose a test duration of 1 second, for the following reason: it enabled us to measure thresholds at all positions during a section of an NTSI within a reasonable amount of time. The psychophysical task has implications for natural vision, because it is important to be able to discriminate small luminance differences. On this long time-scale we can think of, for example, detecting the texture and form of objects. On shorter time scales, as studied in Experiment 3, luminance discrimination is important for, for example, motion detection.

PSYCHOPHYSICAL METHODS

Apparatus

Stimuli were presented with a two-channel Maxwellian-view system (Poot *et al*., 1997). One channel provided the adaptation stimulus (a circular, spatially homogeneous field of 6 deg diameter), onto which the other channel superimposed the test stimulus (a circular field of 20 arcmin diameter). Four fixation dots surrounded the test field. The green LEDs (563 nm, Toshiba TLGD190P) used as light sources were linearized by a photodiode feedback circuit (Watanabe *et al*., 1992) and were driven at a rate of 400 Hz by a 12-bit D/A-converter. We estimated retinal illuminance by the method described by Westheimer (1966). The maximum retinal illuminance that could be obtained was 22.000 Td. Observers' heads were fixated using a headrest.

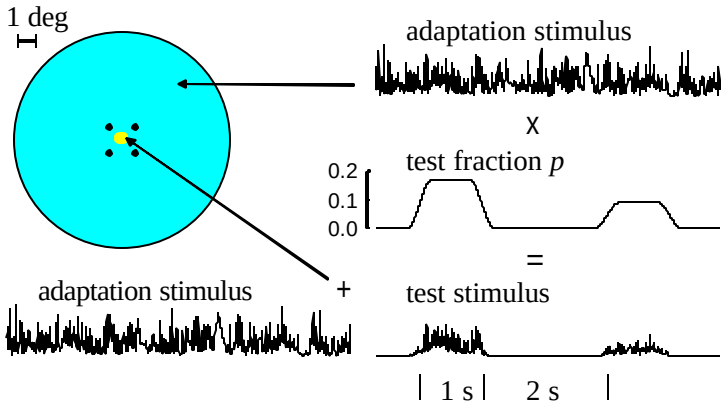

Figure 2. Temporal and spatial structure of the adaptation and test stimuli. The adaptation stimulus (upper row) had a duration of 1 minute, and was shown continuously in the circular adaptation field (diameter 6 deg). Every 3 seconds a test stimulus was shown in the 20-arcmin test field, which was added onto the adaptation field (lower row). The test had luminance dynamics equal to the adaptation stimulus. Test luminance was a fraction *p* of the adaptation luminance, as shown in the middle row. Test duration was 1 second, with smooth 400 ms on- and offset following a cosine taper. The resulting test amplitude (lower row, right column) is drawn here 5 times magnified for clarity. Four fixation dots surrounded the test field.

Psychophysical procedure

As adaptation stimuli we used one minute of an NTSI (van Hateren, 1997), modified versions of the NTSI, and series of pulses. Test stimuli were presented every 3 seconds. The dynamics of the test stimulus was identical to the dynamics of the adaptation stimulus on which it was superimposed; thus during test presentation the test signal was an attenuated copy (a fraction *p*) of the adaptation stimulus (see Fig. 2). The attenuation fraction *p* was varied randomly from presentation to presentation (within a range that was determined by pilot experiments). Above detection threshold, the observer perceived the test stimulus as a homogeneous disc appearing and disappearing smoothly, following the multiplication time-window as can be seen in the middle row in Fig. 2. Observers were asked to assign one of five categories to the visibility of each test presentation (4: perfectly visible, 3: temporally perfectly visible, but spatially blurred, 2: visible, but spatially blurred and temporally fragmented, 1: barely visible, possibly not present, 0: not visible).

In the first experiment, test duration was one second, with on- and offset via a smooth 400 ms cosine taper (i.e. 400 ms onset, 600 ms constant fraction *p*, 400 ms offset). The adaptation stimulus was the NTSI in this experiment. We used 21 test fractions evenly spaced between 0 and 0.2, test fractions were presented randomly with equal probability. In a series of three consecutive runs, with the test window series time-shifted 1 second

in each run, responses (0-4) from each second of the NTSI were collected. These three runs were duplicated five times (5 responses for each second to one test fraction were collected), responses from these five duplications were averaged. As a result we then have for each second an average response value, to a different test fraction. To be able to collect responses to a large range of test fractions for each second, the complete procedure was repeated 20 times. Each repetition provided responses for each second to a different test fraction.

In the second experiment we determined thresholds for several other adaptation stimuli. We pooled responses from different seconds to form one threshold for the complete 1-minute adaptation stimulus. We duplicated each run 3-5 times to give a total of 180-300 responses for each threshold. During each session a range of 8-20 values of test fractions was presented, which were distributed widely and roughly symmetrically around the expected threshold value expected from pilot runs. The experiment was repeated 2-5 times, to obtain higher accuracy.

In the third experiment the same procedure as in the second experiment was followed, but the duration of the test stimulus was decreased (250, 100, 50 and 10 ms). The proportion of the duration of the cosine taper and the duration of the constant period of the test window was kept constant, e.g. a test duration of 100 ms corresponds to a 40 ms cosine taper at onset, a constant period of 60 ms, and a 40 ms cosine taper at offset. In a control experiment we also tested the effect of the steepness of the slope at on- and offset of the test. We determined thresholds for tests with abrupt on- and offset (no cosine taper; a constant test fraction for the complete test duration).

To determine a threshold from the measured responses, a psychometrical curve was fitted to the averaged responses R_{av} as a function of test fraction p, with the following form:

$$R_{av} = 4 \cdot erf\left(0.477 \cdot \left(\frac{p}{p_{th}}\right)^{b}\right). \qquad (1)$$

The definition of this error function was (Press *et al*., 1988):

$$erf(x) = \frac{2}{\sqrt{p}} \cdot \int_0^x e^{-t^2}\, dt\,. \qquad (2)$$

Threshold p_{th} was defined as the test fraction for which the fit yields response category 2 (erf(0.477) = 0.5); b determines the steepness of the psychometrical curve. In the case were responses were pooled, we also determined this parameter b.

Observers

Five observers (age 25-39 years; 3 male, 2 female) took part in this study. All observers were aware of the goal of this study and had experience with psychophysical

experiments. Two observers had good acuity, three were corrected to normal for refractive errors.

RESULTS

Experiment 1

In a first experiment, two observers measured thresholds for each second of the NTSI separately. Thresholds for two observers are shown in Fig. 3. The distribution of thresholds is quite narrow (standard deviation 12% of the mean), and there was virtually no correlation between the observers (r = -0.002). Therefore, we decided not to measure thresholds for each second separately in further experiments, but to pool responses from different seconds in order to calculate one threshold for the complete 1-minute. In this way we obtained thresholds for three additional observers. Threshold for the NTSI (p_{th} = 0.087, average of five observers), was elevated only about 30% above the threshold for a steady, non-modulated adaptation stimulus (p_{th} = 0.067). We can therefore conclude that the visual system handles this stimulus very well, and does not seem to become saturated by large intensity fluctuations.

Experiment 2

In order to compare threshold for the NTSI with thresholds for stimuli with different dynamics, we measured thresholds for the NTSI raised to various powers (0, 0.5, 1.5, 1.75, 2). Examples of a single second of these stimuli are shown in Fig. 4A. These time series range from completely constant (for power 0) to sharply peaked, while all have equal average luminance (1400 Td). With increasing power, both stimulus contrast and slow luminance variations increase in magnitude.

Thresholds to these stimuli vary approximately linearly with power coefficient (correlation r = 0.99). This is also the case if thresholds are plotted as a function of contrast (Fig. 4B, filled circles). As a measure for the contrast in the stimuli we here use average rms-contrast, C_{av}. This is calculated per second by first low-pass filtering the signal with a 3 dB cut-off frequency f_c = 24 Hz, and then dividing the standard deviation of each second by its mean. The cut-off frequency is based on the results of Kelly (1961). This procedure gives $C_{av} = 0.41 \pm 0.20$ (s.d.) for the NTSI.

The thresholds reported in Fig. 4B are the geometric means of all the individual determinations collected for all the observers (using the arithmetic mean does not affect our conclusions):

$$p_{th} = \left(\prod_{i=1}^{N} p_{th,i} \right)^{\frac{1}{N}}, \qquad (3)$$

with N = 8 - 37, depending on the condition. The errors in the thresholds plotted were estimated as follows: we determined the standard deviation of a set of 14 thresholds

measured by one observer (LP) for one stimulus condition. This value was 10.4 % of threshold. The error bars in Fig. 4B are SEMs based upon this estimate:

$$SEM = \frac{0.104 \cdot p_{th}}{\sqrt{N}} . \qquad (4)$$

We used this method of error estimation (instead of basing the error estimation on the standard deviation of the distribution of all thresholds measured by the different observers for each stimulus condition) because in this way we rule out systematic differences in the sensitivity of the different observers. The standard deviation of Weber fractions for our five observers is about 20 percent of the mean. This value is quite large relative to the random errors shown in Fig. 4 B (2-4%).

The increase of threshold with contrast as shown in Fig. 4 B suggests that it is the contrast of the stimulus that mainly determines the threshold. However, it is also possible that the threshold is mainly determined by the size of luminance steps, which also increases with the power coefficient (see Fig. 4 A). In earlier experiments with step-like stimuli (Poot *et al*., 1997), we found large threshold elevations both due to the initial contrast of the flank and due to the plateau luminance of positive luminance steps.

In order to investigate separately the role of luminance and contrast mechanisms, we designed:

1. LPF: an NTSI low-pass filtered at 1.2 Hz, with diminished contrast (C_{av} = 0.20 ± 0.14), but slow luminance variations intact (Fig. 4 A).
2. SHUF: a time series with all 10 ms segments of the NTSI shuffled in random order, with contrast slightly larger (C_{av} = 0.44 ± 0.05) than that of the NTSI, but with negligible slow luminance variations.
3. BIP: a 6.25 Hz bipolar pulse series (average luminance identical to that of the NTSI, with each pulse consisting of a positive lobe of 25 ms at twice that luminance, immediately followed by a negative lobe of 25 ms at zero luminance), with contrast slightly larger than that of the NTSI (C_{av} = 0.44), but with minimal slow luminance variations.

The results for these stimuli (Fig. 4 B, crosses) are fully consistent with the results of the power-transformed NTSIs, when plotted as a function of contrast. Thresholds for BIP and SHUF are elevated, in accordance with the hypothesis that this is caused by their contrast, and not by large luminance steps (which are absent in the BIP and SHUF). Threshold for the LPF series is almost equal to that of the series with power coefficient 0.5, with both stimuli having equal contrast, but the LPF series having considerably larger slow luminance variations. Threshold for the LPF series is, however, not statistically significantly different from that for the NTSI, the value that it would have when slow luminance variations would cause threshold elevation. From the first control experiments with BIP and SHUF we conclude that contrast adaptation is a limiting factor

in this experiment, but luminance adaptation is not. Threshold for the LPF series further substantiates this conclusion.

Experiment 3

The purpose of Experiment 3 was to test if and how the relation between threshold and contrast is influenced by the duration of the test window. Thresholds for test durations t of 10, 50, 100, 250 and 1000 ms were measured. Results for one observer are shown in Fig. 5. A second observer measured thresholds for a selection of the stimulus conditions shown in Fig. 5; results were similar. Thresholds are plotted as a function of power coefficient, since determining a correct value of stimulus contrast becomes increasingly difficult when the test window becomes shorter. The previously used values do no longer apply, since local contrast can change within a period of 1 second, and the exact placement of the shorter test within this period becomes important. But when we calculate contrast for shorter test windows, low-frequency fluctuations do not contribute to contrast any longer. For the 1-minute natural time series filtered at 24 Hz this causes a decrease in contrast by a factor of 7.6 between average rms-contrast calculated from stretches of 1 s and that calculated from stretches of 10 ms. The difference between contrast for the complete 1-minute time series and the average contrast from stretches of 1 second is less dramatic; it is only a factor of 1.5.

The lines drawn in Fig. 5 are linear least-squares fits to the data. The increase in the slope of the curves with shorter test times can clearly be seen; we estimate a difference in slope between the curve for 10 ms tests and 1-s tests of about a factor of 3. Thresholds increase with decreasing test duration, and the rate with which this happens depends on the power coefficient (which is correlated with contrast). The effect of test duration is smallest for power coefficient 0 (a constant adaptation stimulus), and increases with increasing power coefficient (contrast). The 10 ms threshold curve is raised considerably as a whole as would be expected from Bloch's law.

In a control experiment we tested whether or not the cosine-taper at the on- and offset of the test window influences thresholds. For this we compared the thresholds obtained for the cosine-tapered test windows with thresholds measured for an abrupt on-and offset (rectangular test window). Test durations in this experiment were 10, 50, 100 and 1000 ms. The test with a cosine taper and that with abrupt on- and offset gave similar thresholds for the 3 stimulus conditions measured (power 0, 1 and 2). The observer was only able to determine which kind of test was presented in the low-contrast stimulus condition (power 0).

As a second control we estimated the variability of thresholds at different moments in the adaptation stimulus. Since we do not have enough responses to calculate a threshold for each test position separately, we used an indirect method. The slope b of the fitted psychometrical curve gives an indication of this variability. Variation of threshold with test position will cause the slope of the psychometrical curve to decline, when data are pooled over different test positions, as in the present experiment (Hallet, 1969). We calculated average values of b for all stimulus conditions at each test duration. This value did not decline substantially with declining test durations ((t, b) = (1000,2.7),

(250,2.6), (100,2.5), (50,2.8), (10,2.0)). For test durations $\tau \geq 50$ ms, we can thus infer that thresholds at shorter test durations do not vary more than the longest (1000 ms) test duration reported in Fig. 3.

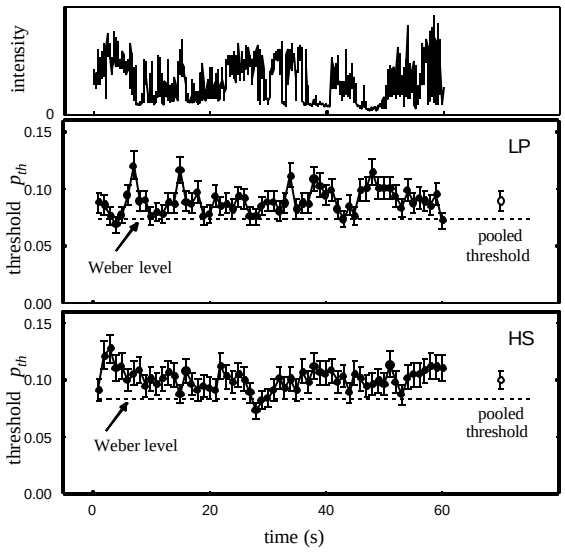

Figure 3. Thresholds p_{th} (filled circles) for observer, LP and HS for each second of the 1-minute NTSI. The open circles show the thresholds (mean ± s.d.) calculated from the pooled responses from all different seconds. The dotted lines show thresholds for a steady background (Weber level). In the top, the NTSI intensity is shown on the same time-scale. Thresholds for the NTSI are elevated only slightly above Weber level. There is no clear correlation between thresholds and NTSI.

DISCUSSION

The main results of the first two experiments of this study are, first, that thresholds for natural time series of intensities are elevated only little above steady-state level; second, that for these and other adaptation stimuli tested, threshold varies approximately linearly with stimulus contrast; and third, that the particular luminance dynamics of adaptation stimuli with identical contrast does not appear to influence threshold.

These results are consistent with the neural processing expected from the spatio-temporal characteristics of the test stimulus. Contrast detection is mediated by separate processing pathways in the visual system, namely the parvocellular (PC) and magnocellular (MC) pathways, which are tuned to different spatial and temporal characteristics (Derrington & Lennie, 1984; Purpura *et al.*, 1990). In Experiments 1 and 2, the PC pathway can be expected to mediate detection of the test stimulus, since this pathway is tuned to low temporal frequencies and high spatial frequencies, and the test has smooth on- and offset, a long duration, and a sharp spatial edge. The analysis below suggests that detection of the test stimulus is most likely mediated by the PC pathway.

Recently, Pokorny and Smith (1997) developed a model for psychophysical contrast discrimination, which is based on the physiological data for neurons in the PC and MC pathway (their Eq. 3). In his comment to the Pokorny & Smith paper, Snippe (1998) deduced a model with fewer parameters (his Eqs. 3 and 4), which described their data equally well. In this model, the slope of the threshold curve depends only on the neuronal half-saturating contrast C_{sat}, whereas the vertical placement of the curve depends on the contrast gain R_{max} / C_{sat} (R_{max} is the maximum neuronal firing rate). Expressing Snippe's Eq. (4) in the present parameters yields

$$p_{th} = p_{th,0} \cdot \left(1 + \frac{C_{av}}{C_{sat}} \right)^2 , \tag{5}$$

where $p_{th,0}$ is the threshold for zero stimulus contrast. A fit of Eq. 5 to our data is shown in Fig. 4 B with C_{sat} = 3.1 (an error analysis yields an estimate C_{sat} = 3.1 ± 0.2). Although this value is larger than the value that Kaplan & Shapley (1986) deduce from their physiological measurements of parvocellular LGN cells in macaque (1.23 in terms of rms-contrast), our value is in fact consistent with their data. We found that various pairs of C_{sat} and R_{max} (e.g., {1.23, 45}, {2,70}, {3.1, 105}, and {4, 130}) provide good fits to their measurements. All these maximum spike rates, R_{max}, are within a physiologically plausible range (Hicks et al., 1983; Sclar et al., 1990; Berry & Meister, 1998; Burkhardt et al., 1998). Furthermore, the value of R_{max} is a value that will probably not be reached when using sinusoidally flickering stimuli for stimulation of parvocellular cells, since the contrast peaks of a sinusoid are too low to stimulate the cells maximally.

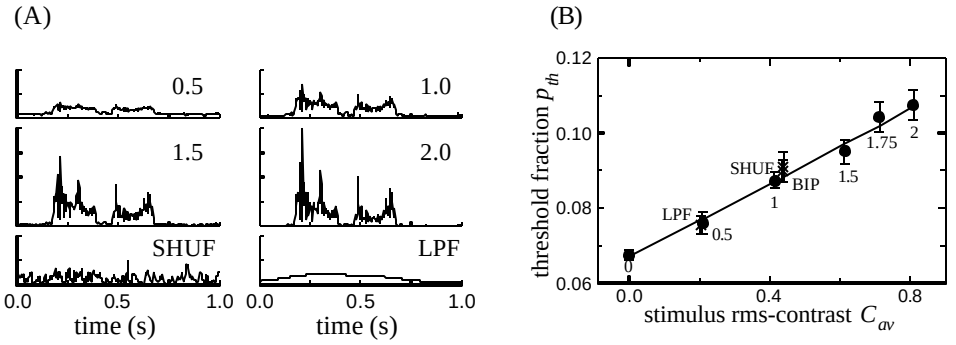

Figure 4. (A) Examples of 1-second segments of several adaptation stimuli. The four upper graphs are the NTSI raised to various powers (0.5, 1, 1.5, 2). Power 1 shows the original time series. The two bottom graphs show a time series of randomly shuffled 10 ms segments of the natural time series (SHUF), and a low-pass filtered NTSI (LPF). (B) Thresholds for the different adaptation stimuli, plotted as a function of stimulus rms-contrast. Filled circles are thresholds, p_{th}, for the time series raised to various powers (0, 0.5, 1, 1.5, 1.75, 2), crosses are thresholds for the three other adaptation stimuli (LPF, SHUF, BIP). BIP is a series of bipolar pulses; see text for details. Error bars indicate SEM

for 4-5 observers. The line is a fit to the data using the model developed by Pokorny and Smith (1997) for psychophysical contrast discrimination, following Eq. (4) of Snippe (1998).
Our data are more difficult to describe by a model of the MC-pathway, since saturation in that pathway already occurs at contrasts as low as about 0.1 (Kaplan & Shapley, 1986, Sclar *et al*., 1990). We then would have found a large increase in threshold already at small contrasts. Even for a 12.5 Hz pulse series with high contrast (pulses of duration 15 ms and illuminance 7950 Td and illuminance 0 between pulses; C_{av} = 1.46), thresholds did not indicate saturation of the pathway mediating detection (p_{th} = 0.114 ± 0.006). This value differs significantly from the curve fitted in Fig. 4 B, which is probably caused by the fact that, for this stimulus, the estimation of contrast depends strongly on the choice of the cut-off frequency f_c of the low-pass filter used in our definition of stimulus contrast ({f_c, C_{av}}= e.g.{5.8, 0.27}, {16, 1.19}, {24, 1.46}, and {200, 2.08}), whereas this dependence is considerably less for the natural time series ({f_c, C_{av} }= {5.8, 0.34}, {16, 0.39}, {24, 0.41}, and {200, 0.50}), and the transformed time series with power 2 (e.g. {f_c, C_{av} }= {5.8, 0.64}, {16, 0.76}, {24, 0.81}, and {200, 1.0}). The value of C_{sat} estimated using the power transformed natural time series is therefore only slightly influenced by the choice of f_c.

Pokorny & Smith (1997) estimate a $C_{sat} \approx 1$ (Weber contrast; rms-contrast ≈ 0.24) for the results in their Fig. 4. A possible explanation for this appreciably lower value than we find here lies in differences between stimulus paradigms. First, the paradigms are temporally quite different: we use a continuously present adaptation stimulus, while theirs (1 raised cosine cycle) is only present for 1.5 seconds, simultaneously with the test. This could result in a steeper contrast-threshold curve because of transients due to the sudden onset of contrast. Second, there are considerable differences in the spatial layout and size of the test and adaptation fields.

The results from our first two experiments suggest that for long (1 s) test stimuli, test detection during natural luminance and contrast variations is mediated by the PC pathway. In the third experiment the test duration was decreased. The results in Fig. 5 show an increase in the slope of the threshold curves with shorter test durations.

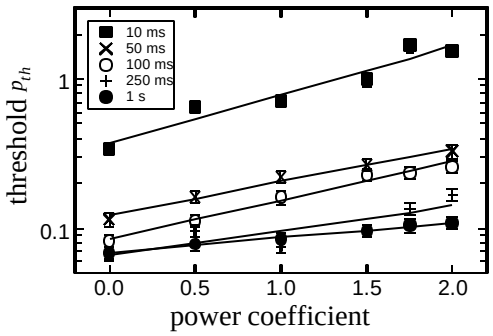

Figure 5. Thresholds p_{th} of observer LP for the power-transformed NTSIs plotted as a function of power (0, 0.5, 1.0, 1.5 and 2.0). The different symbols denote the different test durations (10, 50, 100, 250 and 1000 ms) as indicated in the legend. The drawn lines are linear least squares fits of the plotted data.

Surprisingly, the increase is rather small. This might indicate that test detection is still mostly mediated by the PC pathway also for these shorter test durations. However, we have not fitted these data with the contrast model used in Experiment 2 (Fig. 4 B) for two reasons. First, as mentioned earlier, it is not possible to unambiguously assign a contrast to each stimulus at shorter test durations, and thus it is not possible to calculate a reliable value of C_{sat} for these curves. Second, we are not certain that these curves can be fitted with only one model curve. It is not known if and how the MC pathway takes over from the PC pathway at shorter test durations. We can expect that with shorter test durations the situation becomes more and more advantageous for the MC pathway because of its tuning to higher temporal frequencies (Derrington, 1984). It is possible, however, that for high-contrast stimuli the PC pathway mediates detection down to shorter test durations than it does for low-contrast stimuli. This is expected from the fact that the MC pathway saturates at lower contrasts than the PC pathway. This would mean a transition from one pathway to the other within one threshold curve. Since we do not see a clear transition within one curve, the two pathways possibly link up smoothly. More extensive experiments are needed to elucidate the role of the PC and MC pathway in the psychophysical detection experiments.

Finally, we discuss here the way in which the NTSI is presented during the psychophysical experiments, and the implications for the interpretation of the results presented. The NTSI is presented in a spatially homogeneous way, which is clearly not the natural situation. As mentioned in the Introduction, we present the NTSI in this way for two reasons. First, to obtain a well-defined adaptation condition for each photoreceptor in an appreciable part of the visual field, such that the adaptation does not depend on possible eye-movements during the experiment. Second, spatial display equipment which can handle the full dynamic range of the NTSI is not yet available, thus this is the only practical stimulus we can present. How does this affect the psychophysical results presented in this paper? Each separate photoreceptor does receive the correct input, but the spatio-temporal correlations between photoreceptor inputs are not as they are in natural circumstances. In the following we discuss to what extent this difference would affect the adaptation condition of the visual system beyond the photoreceptor inputs. Traditionally, luminance adaptation has been separated into divisive (or multiplicative) and subtractive components (Hayhoe *et al.*, 1987). Psychophysical evidence indicates that divisive luminance adaptation occurs locally in the retina. Divisive gain control is performed very locally, close to the scale of a cone's receptive field (Chaparro *et al.*, 1995; He & MacLeod, 1998). Thus we expect that the divisive component of luminance adaptation remains natural also for our spatially homogeneous presentation. Furthermore, anatomical data show that in the retina the parvocellular pathway remains spatially very localized (Dacey, 1993; Lee, 1996). Each PC ganglion cell receives direct input from only one midget bipolar cell, which, in turn, receives direct input from only one photoreceptor.

An important mechanism mediating subtractive luminance adaptation is due to the center-surround structure of the spatial receptive fields of bipolar and ganglion cells (Hayhoe, 1990; Werblin, 1974; Enroth-Cugell & Lennie, 1975). The size of the surround field is larger than the center size, due to pooling of receptor inputs. However, for the surround it does not make a large difference if the background is homogeneous or not, if only the average luminance over the surround field is about the same in both conditions. In natural images, there is a large spatial correlation between luminance values of pixels and their neighbours, and this correlation only slowly decreases with larger distances (Ruderman, 1997). It is therefore not unreasonable to assume a roughly even luminance for the small area of a typical PC cell surround field (Lee, 1996). Thus the use of a homogeneous background, instead of a fully naturalistic spatio-temporal input, may have only a limited effect on luminance adaptation in the PC pathway.

For the magnocellular pathway the situation is less clear. MC ganglion cells have receptive fields larger than PC ganglion cells, and they receive direct input from several parasol bipolar cells, which in turn receive input from multiple cones (Perry et al., 1984). Therefore, effects of the spatial structure of the background on luminance adaptation in the MC pathway can be expected to be larger than in the PC pathway. A further important process is contrast gain control, which affects MC ganglion cells, but not PC ganglion cells (Benardete *et al*., 1992; Lee *et al*., 1994). Insofar that contrast gain is driven by spatial contrast, in addition to temporal contrast, further effects of the spatial structure of the stimulus can be expected for the MC pathway. To describe these effects, more detailed information about the contrast gain control is needed.

In the present discussion we argue that detection of the 1-second test is most likely mediated by the PC pathway. If this is the case, the influence of the absence of spatial structure in our experiments may be limited. For shorter test durations we expect a larger contribution of the MC pathway, and thus more influence from the spatial structure of the background. Eventually, it is therefore necessary to perform experiments with spatio-temporal paradigms, if we want to draw conclusions about the role of the MC pathway in natural vision.

ACKNOWLEDGEMENTS

We thank Marten Jansen and Esther Wiersinga-Post for serving as observers, Arjen van der Schaaf for suggesting the use of power-transformed NTSIs, and Kees Schilstra and Esther Wiersinga-Post for comments on the manuscript. This research was supported by the Netherlands Organisation for Scientific Research.

REFERENCES

Benardete, E.A., Kaplan, E. & Knight, B.W. (1992). Contrast gain control in the primate retina: P cells are not X-like, some M cells are. *Visual Neuroscience* **8**, 483-486.

Berry, M.J. & Meister, M. (1998). Refractoriness and neural precision. *Journal of Neuroscience* **18**, 2200-2211.

Burkhardt, D.A., Fahey, P.K. & Sikora, M. (1998). Responses of ganglion cells to contrast steps in the light-adapted retina of the tiger salamander. *Visual Neuroscience* **15**, 219-229.

Carpenter, R.H.S. (1977). *Movements of the eyes*. London: Pion Limited.

Chaparro, A., Stromeyer III, C.F., Chen, G. & Kronauer, R.E. (1995). Human cones appear to adapt at low light levels: measurements on the red-green detection mechanism. *Vision Research* **35**, 3103-3118.

Cornilleau-Pérès, V. & Gielen, C.C.A.M. (1996). Interactions between self-motion and depth perception in the processing of optic flow. *Trends in Neurosciences* **19**, 196-202.

Dacey, D.M. (1993). The mosaic of midget ganglion cells in the human retina. *The Journal of Neuroscience* **13**, 5334-5355.

Derrington, A.M. & Lennie, P. (1984). Spatial and temporal contrast sensitivities of neurones in lateral geniculate nucleus of macaque. *Journal of Physiology* **357**, 219-240.

Donner, K., Copenhagen, D.R. & Reuter, T. (1990). Weber and noise adaptation in the retina of the toad *Bufo marinus*. *Journal of General Physiology* **95**, 733-753.

Enroth-Cugell, C. & Lennie, P. (1975). The control of retinal ganglion cell discharge by receptive field surrounds. *Journal of Physiology, London* **247**, 551-578.

Epelboim, J. (1998). Gaze and retinal-image stability in two kinds of sequential looking tasks. *Vision Research* **38**, 3773-3784.

Foley, J.M. & Boynton, G.M. (1993). Forward pattern masking and adaptation: effects of duration, interstimulus interval, contrast, and spatial and temporal frequency. *Vision Research* **33**, 959-980.

Grasso, R., Prévost, P., Ivanenko, Y.P. & Berthoz, A. (1998). Eye-head coordination for the steering of locomotion in humans: an anticipatory synergy. *Neuroscience Letters* **253**, 115-118.

Hallet, P.E. (1969). The variations in visual threshold measurement. *Journal of Physiology, London* **202**, 403-419.

van Hateren, J.H. (1997). Processing of natural time series of intensities by the visual system of the blowfly. *Vision Research* **37**, 3407-3416.

Hayhoe, M.M., Benimoff, N.I. & Hood, D.C. (1987). The time course of multiplicative and subtractive adaptation processes. *Vision Research* **27**, 1981-1996.

Hayhoe, M.M. (1990). Spatial interactions and models of adaptation. *Vision Research* **30**, 957-965.

Hayhoe, M.M., Levin, M.E. & Koshel, R.J. (1992). Subtractive processes in light adaptation. *Vision Research* **32**, 323-333.

He, S. & MacLeod, D.I.A. (1998). Contrast-modulation flicker: dynamics and spatial resolution of the light adaptation process. *Vision Research* **38**, 985-1000.

Hicks, T.P., Lee, B.B. & Vidyasagar, T.R. (1983). The responses of cells in macaque lateral geniculate nucleus to sinusoidal gratings. *Journal of Physiology* **337**, 183-200.

Hood, D.C., Graham, N., von Wiegand, T.E. & Chase, V.M. (1997). Probed-sinewave paradigm: a test of models of light-adaptation dynamics. *Vision Research* **37**, 1177-1191.

Kaplan, E. & Shapley, R.M. (1986). The primate retina contains two types of ganglion cells, with high and low contrast sensitivity. *Proceedings of the National Academy of Sciences USA* **83**, 2755-2757.

Kelly, D.H. (1961). Visual responses to time-dependent stimuli. I. Amplitude sensitivity measurements. *Journal of the Optical Society of America* **51**, 422-429.

Koenderink, J.J. (1986). Optic flow. *Vision Research* **26**, 161-180.

Kortum, P.T. & Geisler, W.S. (1995). Adaptation mechanisms in spatial vision-II. Flash thresholds and background adaptation. *Vision Research* **35**, 1595-1609.

Kowler, E., Pizlo, Z., Zhu, G., Erkelens, C.J., Steinman, R.M. & Collewijn, H. (1992). Coordination of head and eyes during the performance of natural (and unnatural) visual tasks. In Berthoz, A., Vidal, P.P. & Graf, W. (Eds*), The head-neck sensory motor system* (pp. 419-426). New York: Oxford University Press.

Lankheet, M.J.M., van Wezel, R.J.A., Prickaerts, J.H.H.J. & van de Grind, W.A. (1993). The dynamics of light adaptation in cat horizontal cell responses. *Vision Research* **33**, 1153-1171.

Lee, B.B., Pokorny J., Smith, V.C., Kremers, J. (1994). Responses to pulses and sinusoids in macaque ganglion cells. *Vision Research* **34**, 3081-3096.

Lee, B.B. (1996). Receptive field structure in the primate retina. *Vision Research* **36**, 631-644.

Perry, V.H., Oehler, R. & Cowey, A. (1984). Retinal ganglion cells that project to the dorsal lateral geniculate nucleus in the macaque monkey. *Neuroscience* **12**, 1101-1123.

Pokorny, J. & Smith, V.C. (1997). Psychophysical signatures associated with magnocellular and parvocellular pathway contrast gain. *Journal of the Optical Society of America A* **14**, 2477-2486.

Poot, L., Snippe, H.P. & van Hateren, J.H. (1997). Dynamics of light adaptation at high luminances: adaptation is faster after luminance decrements than after luminance increments. *Journal of the Optical Society of America A* **14**, 2499-2508.

Press, W.H., Teukolsky, S.A., Vetterling, W.T. & Flannery, B.P. (1988). *Numerical Recipes in C: the Art of Scientific Computing*. Cambridge: Cambridge University Press.

Purpura, K. Tranchina, D., Kaplan, E. & Shapley, R.M. (1990). Light adaptation in the primate retina: analysis in gain and dynamics of monkey retinal ganglion cells. *Visual Neuroscience* **4**, 75-93.

Ruderman, D.L. (1997). Origins of scaling in natural images. *Vision Research* **37**, 3385-3398.

Sclar, G., Maunsell, J.H.R. & Lennie, P. (1990). Coding of image contrast in central visual pathways of the macaque monkey. *Vision Research* **30**, 1-10.

Shapley, R.M. & Enroth-Cugell, C. (1984). Visual adaptation and retinal gain controls. *Progress in Retinal Research* **3**, 263-343.

Shapley, R.M. (1997). Adapting to the changing scene. *Current Biology* **7**, R421-R423.

Snippe, H.P. (1998). Psychophysical signatures associated with magnocellular and parvocellular pathway contrast gain: comment. *Journal of the Optical Society of America A* **15**, 2440-2442 .

Victor, J.D., Conte, M.M. & Purpura, K.P. (1997). Dynamic shifts of the contrast-response function. *Visual Neuroscience* **14**, 577-587.

Watanabe, T., Mori, N. & Nakamura, F. (1992). A new superbright LED stimulator: photodiode-feedback design for linearizing and stabilizing emitted light. *Vision Research* **32**, 953-961.

Werblin, F. (1974). Control of retinal sensitivity. *Journal of General Physiology* **63**, 62-87.

Wu, S. & Burns, S.A. (1996). Analysis of retinal light adaptation with the flicker electroretinogram. *Journal of the Optical Society of America A* **13**, 649-657.

Chapter 4

Yeh, T., Lee, B.B. & Kremers, J. (1996). The time course of adaptation in macaque retinal ganglion cells. *Vision Research* **36**, 913-931.